

HIGH RESOLUTION ELECTRON MICROSCOPY OF FELDSPAR WEATHERING

RICHARD A. EGGLETON

Geology Department, Australian National University
P.O. Box 4, Canberra, ACT 2600, Australia

PETER R. BUSECK

Departments of Chemistry and Geology, Arizona State University
Tempe, Arizona 85281

Abstract—High resolution imaging by transmission electron microscopy has revealed a mechanism for the weathering of intermediate microcline in a humid, temperate climate. Dissolution of the feldspar begins at the boundary of twinned and untwinned domains and produces circular holes which enlarge to form negative crystals. Amorphous, ring-shaped structures develop, about 25 Å in diameter, within the larger holes. These rings, in turn, crystallize to an arcuate phase having a 10-Å basal spacing and then to crinkled sheets of illite or dehydrated montmorillonite. The 10-Å layer silicate shows an irregular stacking sequence, including 10-, 20-, and 30-Å sequences. Included plagioclase crystals show a similar mechanism of weathering and, moreover, are more intensely weathered.

Key Words—Feldspar, Illite/montmorillonite, Ion thinning, Microcline, Transmission electron microscopy, Weathering.

INTRODUCTION

The weathering products of feldspar are the major constituents of soil. Whereas there have been extensive studies of feldspar weathering in bulk samples and a great deal is known about the chemistry of the process and its end products, relatively little is known about the earliest stages of feldspar breakdown. The present study uses the methods of high-resolution transmission electron microscopy (HRTEM) to investigate feldspar weathering at its onset, before the reaction products have reached the degree of crystallinity and crystal size necessary for identification by X-ray diffraction or other bulk methods.

Petrović (1976), in his discussion of rate control in feldspar dissolution, summarized results obtained in aqueous solution over a range of pH and temperature. The alteration phases found in such experiments are aluminosilicate gel particles, <200 Å in diameter, and the crystalline products gibbsite, fibrous boehmite, kaolinite, and halloysite.

Weathered feldspar develops a brownish “turbid” appearance, very familiar to optical microscopists. Folk (1955) suggested that turbidity resulted from the development of sub-micrometer size vacuoles. This form of alteration develops at some distance from visible cleavages or cracks within the body of the feldspar, where flowing water cannot penetrate; thus it is evident that weathering does not only proceed from exposed surfaces. The clay minerals that ultimately form during feldspar weathering must owe their origin to the processes occurring at this early stage.

Scanning electron microscopy of weathered feldspar grains (Parham, 1969; Berner and Holdren, 1977; Keller 1976, 1978; Nixon, 1979) shows that crystallographically controlled solution pits form on the surface of feldspar as it weathers. Keller (1976) stated: “Micro-pitting of feldspar, presumably by incongruent dissolution, is a common pre- or early-stage, of kaolinization of feldspar.” Berner and Holdren (1977) expressed “. . . no doubt . . . that the dissolution of feldspar proceeds by selective etching of the surface, probably along dislocations.”

Suttner *et al.* (1976) concluded that kaolin forms from feldspar under humid conditions, whereas smectite forms in semi-arid climates, the difference resulting from more complete flushing of K⁺ ions under humid weathering. Vacuoles occur in all of their optically examined material, but are most prominent in the western arid samples. They also found that plagioclase altered more rapidly, or more extensively, than microcline.

EXPERIMENTAL

Sample

The feldspar selected for this investigation was from a suite of perthitic K-feldspar megacrysts from the Kameruka granodiorite in southern New South Wales, Australia. These crystals have been the subject of an extensive study (Eggleton, 1979). By examining such well known material, it is easier to separate weathering effects from phenomena associated with the feldspar's earlier igneous history. The weathering took place in a humid climate, with an annual rainfall of about 1000

Table 1. Chemical analyses of feldspars.

	ABF28	ABF67	Ksp/Ill
SiO ₂	64.9	60.5	60.6
Al ₂ O ₃	18.6	23.5	23.3
K ₂ O	15.8	14.2	14.0
Na ₂ O	0.7	0.9	0.5
H ₂ O	—	—	1.5
Total	100.0	99.1	99.9

ABF 28 = Microcline.

ABF 67 = Weathered microcline.

Ksp/III = Calculated composition for a mixture of 72% ABF 28 and 28% illite.

mm and a temperature range of 0°–40°C. Sample ABF28 was collected from a cut at the north end of the Brogo Dam wall, where the granodiorite is heavily weathered and decomposed. Here, megacrysts 5 to 6 cm long may be picked out by hand. Optical examination showed that all of the megacrysts have unaltered regions, and that some have highly altered turbid regions. Plagioclase crystals within the K-feldspar are everywhere more altered than the host. Analysis by energy dispersive electron microprobe of optically clear areas gave a megacryst composition of Or₉₃, in good agreement with the X-ray diffraction composition of Or₉₄ determined using the relation of Stewart and Wright (1974). X-ray powder diffraction films established that the K-feldspar is an intermediate microcline ($\gamma = 89.66^\circ$). The perthite albite lamellae have a composition of Ab₉₆Or₄; the included plagioclase crystals are An₃₁ at the core and are zoned to An₁₅ at the margin.

Analyses of weathered feldspar are limited by the need to select well polished areas, which automatically excludes severely altered material. The most highly altered microcline analyzed (ABF67 in Table 1) is from a maximum microcline megacryst where Jingo Creek cuts the Wyndham Burragate Road. This analysis shows the expected loss of K₂O and SiO₂ and gain in Al₂O₃ with weathering. The cation proportions of ABF67 correspond closely to an illite: microcline mix in the proportions 28:72, assuming an illite composition of K_{0.67}Al_{2.67}Si_{3.33}O₁₀(OH)₂. Helgeson (1971) showed that at 25°C and high K⁺ activity ($\log(aK^+/aH^+) > 6$), K-mica is in equilibrium with microcline at one atmosphere and unit activity of water.

High resolution transmission electron microscopy

Material selected for examination was taken from 20- μ m thick optical thin sections, and also scratched from areas on megacryst surfaces. Samples were chosen to show a range of weathering, from optically clear through moderately and densely turbid microcline to nearly opaque plagioclase. Sections cut near (001) and (100) were thinned by argon ion bombardment at 5 kV

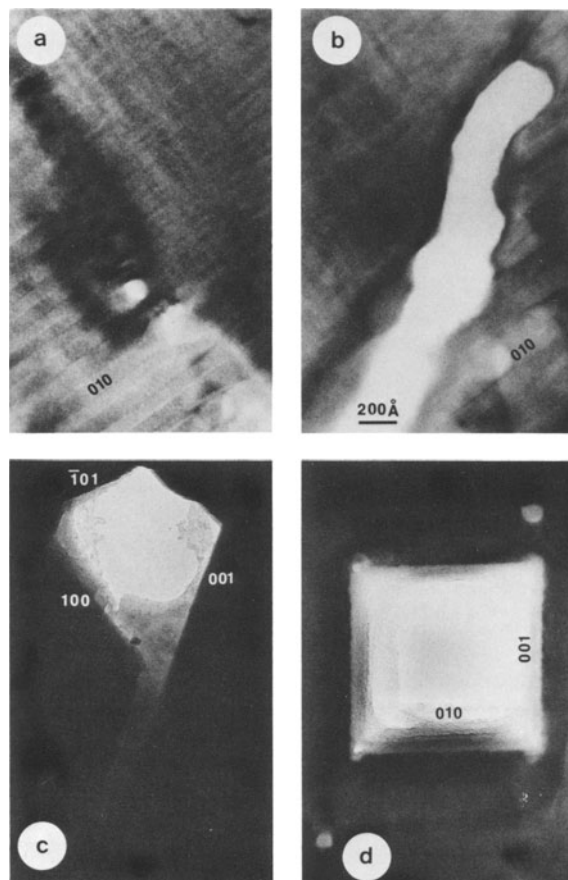


Figure 1. Development of vacuoles. (a) [102] section showing small vacuoles at the boundary between twinned (lower left) and untwinned regions of K-feldspar. (b) Coalescence of vacuoles along a similar boundary region; [102] section. (c) [010] section showing a negative crystal fragment with contained amorphous material. (d) [100] section showing a negative crystal. The scale bar of (b) applies to all four figures.

and 4 μ A, with a final 'cleaning' bombardment at 1 kV for 6 hr. Fragments were also dug from thin sections and from the megacryst surface, crushed, and examined after dispersal on holey carbon films. Observations were made on a JEOL JEM100B electron microscope, operating at 100 kV. The instrumental and experimental conditions and the procedures are those described by Buseck and Iijima (1974) and Veblen and Buseck (1979). The crystals were oriented using a top-entry tilt-rotate stage, and the diffraction patterns indexed using a gold-coated crystal as standard, and confirmed by tilting to other orientations and then relating all observations by stereographic projection. Such standardization is particularly important to insure the distinction between dimensionally similar albite and K-feldspar.

The slightly weathered feldspar examined here is subject to damage by an electron beam to the extent that the time required to tilt a crystal to a desired ori-

entation is considerably greater than the crystal's life expectancy. For ion-milled samples, this poses no particular problem, as the operator can translate to an undamaged area after orientation is achieved. Small fragments are more difficult to orient without damage, and chance orientations were used mostly. The crystalline weathering products are similarly short lived and have generally only been seen in grain mounts. No orientation studies were made of these fragments.

RESULTS

In all but the freshest feldspar, the electron microscope revealed holes, or vacuoles, most commonly in ion-thinned specimens, but also in crushed grains. In an ion-milled specimen, initially 20 μm thick, but viewed after thinning to about 100 \AA , an observed hole is unlikely to be the "actual" hole present before milling, but a hole that was "translated" through the crystal by the milling process itself. Because the ion beam strikes the sample surface at a glancing angle of only 25° or 30°, many surface irregularities will be smoothed out during milling. Even so, it is to be expected that the observed incidence of holes in a particular section will be greater than was originally present in the 100- \AA thick layer exposed to examination. "Translated" holes, if not originally round, will be smoothed and rounded by the milling process, and only holes that are exposed just as milling concludes can be expected to show their true morphology. Similarly, occluded nonfeldspar phases within the holes will only be preserved if they reach the surface as milling concludes.

Many of the vacuoles seen in ion-thinned sections lie at the ends of albite twin lamellae. Interplanar angles measured from Figure 1a and similar photographs showed that the twinned region is close to maximum microcline, whereas the untwinned area is, within experimental error, dimensionally monoclinic. Between these lattices of different geometry must be a region of high strain, or high dislocation density. In fresh feldspar both the orientation changes expected in a strained crystal, and edge dislocations, were seen in such boundary regions. It was therefore concluded that weathering of feldspar commences by the solution of material from these high strain volumes within the crystal. Larger holes are commonly bounded by planes whose traces are parallel to crystallographic directions; thus these holes are negative crystals.

Material showing no diffraction contrast is present within some negative crystals and is accordingly regarded as amorphous material. By electron imaging it is impossible to determine the origin of the lack of crystallinity, whether by ion-beam damage or as the result of weathering. Amorphous material, yielding a broad diffraction halo between 3 and 4 \AA , is common in grain mounts of more highly altered feldspar, and these two amorphous phases can be correlated on a tentative basis.

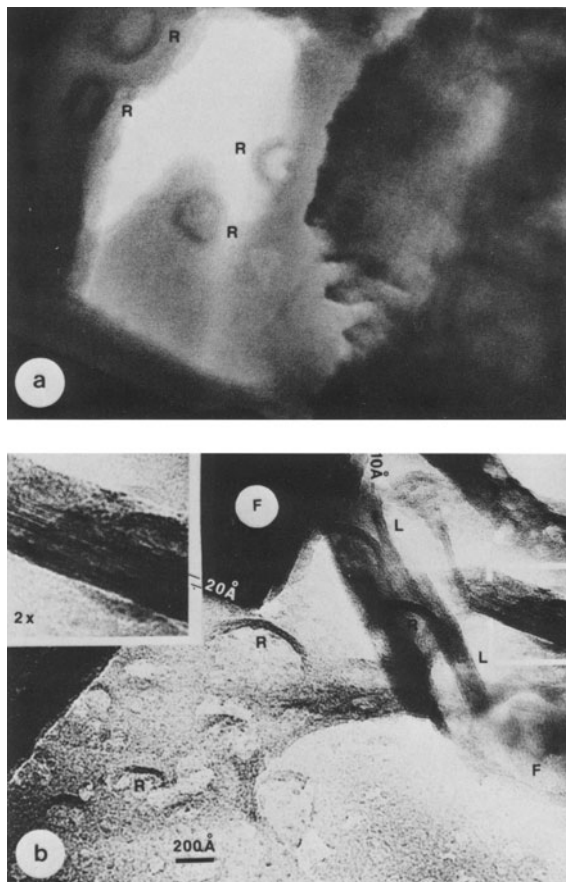


Figure 2. Ring structures (R) and their development to 10- \AA layer silicate. (a) [100] feldspar section, showing a negative crystal with enclosed amorphous material and ring, (R). (b) Fragment suspended on holey carbon film. F = relict feldspar, L = layer silicate with 10- \AA fringes. The framed crystal on the right is enlarged 2 \times on the upper left to reveal the 20- \AA , 2-layer repeat.

In some of the amorphous material, particularly in the holes, ring texture is visible. The rings are about 250 \AA in diameter with a dark (more strongly diffracting) margin (Figure 2a). Under the electron beam, they move slightly, pulsating or "fluttering." By combining observations of sections and crushed grains, a progression can be traced from very unstable, almost structureless rings, to more stable arcuate laths with 10- \AA lattice planes, to a well-crystallized 10- \AA layer silicate (Figure 2b). In other areas there is no evidence for an intermediate ring structure; a poorly to well-crystallized 10- \AA layer silicate occurs directly against, or very close to feldspar (Figure 3).

Figure 4a shows a 3-fringe "bridge" across a vacuole. O'Keefe and Buseck (1979) showed that intuitive identification of high resolution images of silicates is only possible close to optimum defocus (~ 900 \AA for very thin crystals), and even then caution is needed.

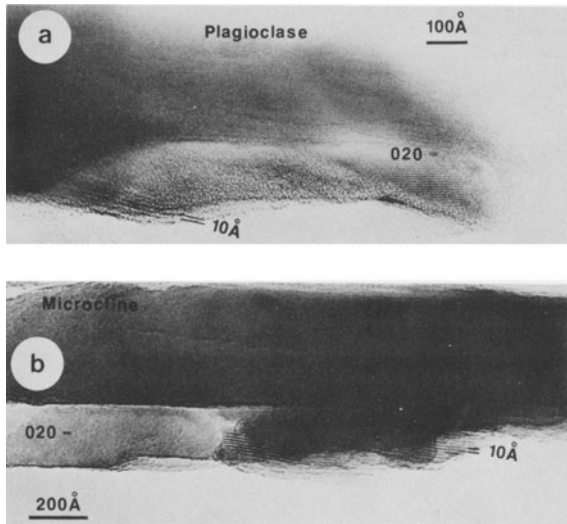


Figure 3. 10-Å layer silicate formed adjacent to feldspar. (a) Plagioclase viewed parallel to (010) showing 6.4-Å (020) fringes and curved 10-Å layer silicate along the lower edge. (b) Comparable microcline crystal with well developed 10-Å phase adjacent.

The wide fringes in Figure 4a are about 16 Å apart, a spacing not found in any feldspar alteration product, except perhaps in fully hydrated montmorillonite, an unlikely survivor in the high vacuum of the microscope. Computation of images to be expected from thin mica crystals (Eggleton and O'Keefe, in preparation) using the methods of O'Keefe and Buseck (1979) shows that at an underfocus of 350 Å, a 2-layer illite crystal, a few unit cells wide and oriented with (001) parallel to the electron beam, can give the image shown in Figure 4b. Such an image could be produced from a curled 2-layer crystal in which the plane of the layer silicate sheet is turned up parallel to the electron beam, but only for a depth of a few unit cells. Many such curled illite sheets have been seen in grain mounts, and, although they are uncommon in ion-thinned crystals, examples such as that shown in Figure 4 reveal that crystallization of alteration products can occur directly in the solution holes.

According to Helgeson (1971), microcline should alter initially to illite or montmorillonite, and plagioclase should alter to montmorillonite. Page and Wenk (1979) found that montmorillonite is an early product in the hydrothermal alteration of plagioclase. Meunier and Velde (1979) reported that "initial weathering in the lowest-massive levels of the (granite) profile produces first illitic mica . . ." Both feldspars studied here show abundant 10-Å phases in their more altered regions (Figures 5, 6). In grain mounts, this phase appears as extremely thin flakes curled at the edges and crinkled or corrugated in several directions (Figure 5a). Projections of these flakes close to [001] shows a regular 4.5-

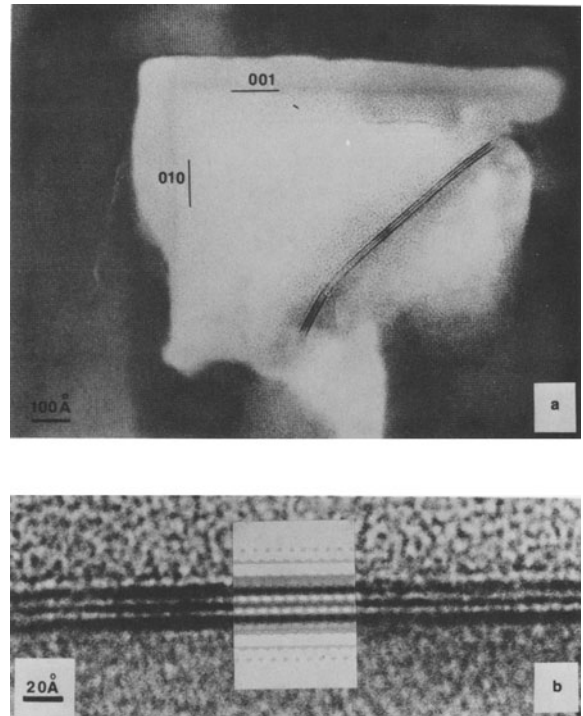


Figure 4. Negative crystal in [100] section of K-feldspar showing 6.4-Å (020) and (001) feldspar-lattice fringes bridged by a crystallite of two sheets of 10-Å layer silicate. (b) The 10-Å layer silicate, at 5 times the magnification of (a), is compared to a computed image calculated at 350-Å under focus from two dioctahedral 2:1 layers with K in $\frac{2}{3}$ of the interlayer sites. At this defocus, the image bears little similarity to the projected charge density of the crystal.

Å hexagonal lattice in a few examples (Figure 5c), but more commonly the xz plane is modulated into linear domains about 10 unit cells across (Figure 6b); lattice rows across domain boundaries change direction by less than 5°. In other flakes subgrains exist only 3 or 4 unit cells wide in any direction. Many examples have been seen of extremely thin (2 or 3 layer) sheets peeling from a substrate having the typical diffraction pattern of a layer silicate a^*b^* section (Figure 6a). Where such sheets curl to present an edge to the electron beam, the layers have been imaged and the 10-Å layer spacing identified in flakes so small that no electron diffraction pattern was detectable. Iijima and Buseck (1978) showed that mica layer sequences can be determined from images obtained from slightly misoriented crystals. Many of the flakes imaged here have 20-Å, 2-layer repeats; many are 1-layer; and others are mixed (Figure 5b).

It is difficult to decide from morphology alone whether a particular crystal is illite, montmorillonite, or muscovite. It seems possible that a complete range through these 10-Å layer silicates is present, the thin crinkled crystal of Figure 6a being montmorillonite, the modu-

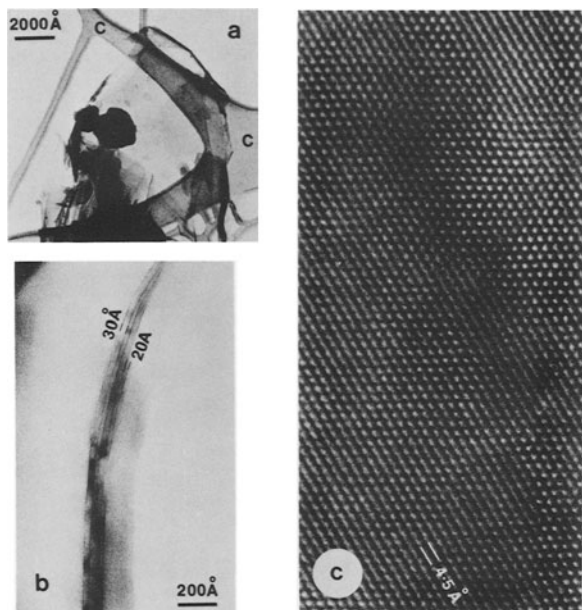


Figure 5. 10-Å layer silicates. (a) Thin crystal having curled edges supported on holey carbon (C). The crystal is crinkled at the lower left, the black blobs are relict feldspar. (b) Curled edge of a flake, showing 2-layer (20 Å) and 3-layer (30 Å) sequences. (c) High magnification image of an unmodulated, slightly wrinkled thin crystal; [001] section.

lated crystal of Figure 6b illite, and the flatter, uniform crystal of Figure 5c 1Md muscovite. At this level of crystallization it is also possible that these distinctions have little meaning, the modulations of one crystal may reflect variations in chemistry across it, giving rise to a 10-Å layer that is "illite" in one area and "montmorillonite" in another. Such modulated structures may be the precursors to interstratified illite/montmorillonite of soils, as the K and Al proportions in a given layer dictate whether it will ultimately become expandable. Alcover *et al.* (1977) described short-range order of the large cations in vermiculitized muscovite, a phenomenon that may be similar to the modulations observed in this study.

Despite extensive searching and examination of more than a thousand micrographs, no evidence has been found for the existence of any other alteration product. In particular, kaolinite or halloysite, gibbsite, or boehmite were sought, but without success. Apparently the movement of water into the regions of feldspar studied was slow enough that the concentrations of K, Na, and Si remained high, and equilibrium was maintained between feldspar and the 10-Å layer silicate. It is unlikely, on the basis of these observations, that the formation of a weathering crust would have any significant effect on the subsequent rate of feldspar weathering to illite or montmorillonite unless such crust were more impervious to water than feldspar itself.

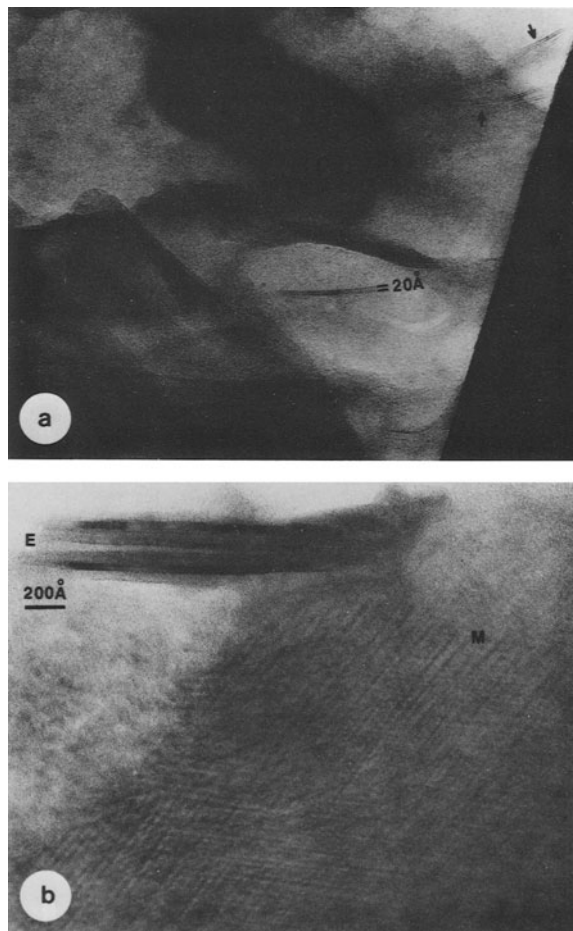


Figure 6. (a) Pairs of 2:1 "tale" layers (arrowed) and a triple (20 Å) sequence peeled up from an unresolved layer-silicate substrate. The dark triangular area on the right is a large feldspar fragment. (b) Layer-silicate crystal (M) with modulations on *ab*, and a curled edge (E) showing 10-Å fringes. The modulations are spaced at about 40 Å; the diameter of the curled edge is about 250 Å.

CONCLUSIONS

Under the weathering conditions studied here, it is not appropriate to consider reactions as occurring simply at the crystal surface, with feldspar inside and reaction product + water outside. Rather, there is an initial reaction between feldspar and diffusing water, beginning at structural defects, and gradually expanding within the crystal. At this early stage, the only crystalline phases are feldspar and 10-Å layer silicate, and it must be assumed from Helgeson's work (1971), that these are in equilibrium. Thus, the beginning of feldspar weathering is, in this instance, an equilibrium process, leading to the formation of an illite/montmorillonite mixed-layer mineral.

ACKNOWLEDGMENTS

We are grateful to Drs. D. Veblen and I. Mackinnon for helpful discussion during the course of this work, and to M. A. O'Keefe for assistance with electron image computations. RAE particularly thanks J. Wheatley for instruction and help in the use of the microscope. The research was supported in part by grant EAR 77-00128 from the Earth Sciences Division of the National Science Foundation.

REFERENCES

- Alcover, S. F., Gatineau, L., Mering, J., and Kodama, H. (1977) The distribution of Ba cations in vermiculite and vermiculitized micas: unpubl. manuscript.
- Berner, R. A. and Holdren, C. R. (1977) Mechanism of feldspar weathering: some observational evidence: *Geology* **5**, 369–372.
- Buseck, P. R. and Iijima, S. (1974) High resolution transmission electron microscopy of silicates: *Amer. Mineral.* **59**, 1–21.
- Eggleton, R. A. (1979) The ordering path for igneous K-feldspar megacrysts: *Amer. Mineral.* **64**, 906–911.
- Folk, R. L. (1955) Note on the significance of turbid feldspars: *Amer. Mineral.* **40**, 356–357.
- Helgeson, H. C. (1971) Kinetics of mass transfer among silicates and aqueous solutions: *Geochim. Cosmochim. Acta* **35**, 421–469.
- Iijima, S. and Buseck, P. R. (1978) Experimental study of disordered mica structures by high resolution electron microscopy: *Acta Cryst.* **A34**, 709–719.
- Keller, W. E. (1976) Scan electron micrographs of kaolins collected from diverse environments or origin—I: *Clays & Clay Minerals* **24**, 107–113.
- Keller, W. E. (1978) Kaolinization of feldspars as displayed in scanning electron micrographs: *Geology* **6**, 184–188.
- Meunier, A. F. and Velde, B. (1979) Weathering mineral facies in altered granites. The importance of small-scale local equilibria: *Mineral. Mag.* **43**, 261–268.
- Nixon, R. A. (1979) Differences in incongruent weathering of plagioclase and microcline—Cation leaching versus precipitates: *Geology* **7**, 221–224.
- O'Keefe, M. A. and Buseck, P. R. (1979) Calculation of the high resolution TEM images of minerals: *Trans. Amer. Cryst. Assoc.* **15** (in press).
- Page, R. and Wenk, H. R. (1979) Phyllosilicate alteration of plagioclase studied by transmission electron microscopy: *Geology* **7**, 393–397.
- Parham, W. E. (1969) Formation of halloysite from feldspar: low temperature artificial weathering versus natural weathering: *Clays & Clay Minerals* **17**, 13–22.
- Petrović, R. (1976) Rate control in feldspar dissolution—II. The protective effect of precipitates: *Geochim. Cosmochim. Acta* **40**, 1509–1521.
- Suttner, L. J., Mack, G., James, W. C., and Young, S. W. (1976) Relative alteration of microcline and sodic plagioclase in semi-arid and humid climates: *Geol. Soc. Amer. Abstracts Programs* **8**, 512.
- Veblen, D. R. and Buseck, P. R. (1979) Chain width order and disorder in biopyriboles: *Amer. Mineral.* **64**, 687–700.

(Received 27 August 1979; accepted 19 December 1979)

Резюме—Высоко разрешающие изображения, полученные трансмиссионной электронной микроскопией, позволили выявить механизм выветривания промежуточного микроклина во влажном умеренном климате. Растворение полевого шпата начинается на границе сдвоенных и несдвоенных доменов, образуя круглые выемки, которые, увеличиваясь, формируют отрицательные кристаллы. В пределах больших выемок образуются аморфные, кольцеобразные структуры около 25 Å в диаметре. Эти кольца, в свою очередь, кристаллизуются в дугообразную фазу, имеющую базальные промежутки в 10 Å и затем в морщинистые листы иллиты или обезвоженного монтмориллонита. 10-Å слоистый силикат проявляет ненормальную последовательность слоев, включая последовательности 10, 20, и 30 Å. Окклюдированные плагиоклазовые кристаллы проявляют сходный механизм выветривания и, к тому же, выветриваются более интенсивно. [N.R.]

Resümee—Die hohe Auflösung, die durch die Transmissionselektronenmikroskopie erreicht wird, zeigt einen Verwitterungsmechanismus von intermediärem Mikroclin in einem humiden, gemäßigten Klima. Die Auflösung von Feldspat beginnt an der Grenze zwischen verzwilligten und nichtverzwilligten Domänen und erzeugt kreisförmige Löcher, die größer werden und negative Kristalle bilden. Es entstehen amorphe, ringförmige Strukturen mit einem Durchmesser von etwa 25 Å in den größeren Löchern. Diese Ringe wiederum kristallisieren zu einer bogenförmigen Phase, die einen Basisabstand von 10 Å hat und anschließend zu runzligen Blättchen aus Illit oder dehydratisiertem Montmorillonit. Das 10-Å-Schichtsilikat zeigt eine unregelmäßige Stapelungsfolge, die 10 Å-, 20 Å- und 30 Å-Folgen beinhaltet. Eingeschlossene Plagioklas-kristalle zeigen einen ähnlichen Verwitterungsmechanismus und sind darüberhinaus intensiver verwittert. [U.W.]

Résumé—Des images à haute résolution obtenues par microscopie à transmission d'électrons ont révélé un mécanisme pour l'altération de la microcline intermédiaire dans un climat humide et tempéré. La dissolution du feldspath commence à la séparation des domaines jumelés et non-jumelés et produit des trous circulaires qui s'agrandissent pour former des cristaux négatifs. Des structures amorphes d'environ 25 Å de diamètre, en forme d'anneau, se développent dans les trous les plus grands. Ces anneaux, à leur tour, se cristallisent en une phase arguée ayant un espacement de base de 10 Å et ensuite en des lames froncées d'illite ou de montmorillonite deshydratée. Le silicate à couches-10 Å montre une séquence irrégulière d'empilement comprenant des séquences de 10, 20, et 30 Å. Des cristaux de plagioclase occlus montrent un mécanisme d'altération semblable, et, de plus, sont plus intensément altérés. [D.J.]